Biointerface Research in Applied Chemistry
Open-Access Journal (ISSN: 2069-5837)

Article
Volume 15, Issue 3, 2025, 34
https://doi.org/10.33263/BRIAC153.034

Thermochemical Effects of Flux and Coke Amount on the Smelting of Low-Grade Chromite Sand to Ferrochrome

Ulin Herlina [1,2,*], Fajar Nurjaman [2,*], Bambang Suharno [1,*], M. Ridwan Al Fahmi [3], Muhammad Syahreyzi Pashey Zulqoernain [3], Febriyani Mesah [3], Anton Sapto Handoko [2] , Hafid Zul Hakim [3], Alio Jasipto [3], Donanta Daneshwara [1], La Ode Arham [3]

[1] Department of Metallurgy and Material, Universitas Indonesia, Depok 16424, Indonesia
[2] Research Center of Mining Technology, National Research and Innovation Agency, Lampung, 35361, Indonesia
[3] Sustainable Mining and Environmental Research Group, Department of Mining Engineering, Institut Teknologi Sumatera, Lampung-35365, Indonesia
* Correspondence: ulin001@brin.go.id (U.H.); faja005@brin.go.id (F.N.); suharno@metal.ui.ac.id (B.S.);
Received: 10.03.2025; Accepted: 10.05.2025; Published: 8.06.2025

Abstract: Ferrochrome serves as a vital ferroalloy product, which functions as a fundamental alloying material in stainless steel production due to its corrosion resistance properties. However, its production needs high-grade chromite ore (46–48% Cr_2O_3) with a chromium-to-iron (Cr/Fe) ratio above 2.8, which creates problems because of declining reserves. To overcome the limitations of low-grade chromite, optimizing process parameters, such as basicity, becomes essential for achieving high metal yield and chromium recovery during smelting. This research investigates how flux type (basicity) and stoichiometric coke amount affect the thermochemical process of low-grade chromite sand (12.43% Cr_2O_3 with a chromium-to-iron ratio of 0,97) smelting using a DC Submerged Arc Furnace (DC SAF), which has a Ø200 mm × 400 mm, powered by a 60V and 100 kVA transformer. The research involved modifying basicity (0.4; 0.6; 0.8; 1; 1.2; 1.4) through silica and limestone flux additions and varying stoichiometric coke addition amounts (0.6; 0.8; 1; 1.2). Material characterizations via XRF, XRD, and SEM-EDX were used to confirm chromite and iron content, phase transformations, and product microstructure. The optimal results were achieved using a basicity of 0.6 with 20% stoichiometric coke addition, which produced 98.72% chromium recovery, 18.33% metal yield, and ferrochrome containing 45.78% chromium. The ferrochrome product meets the minimum low-grade ferrochrome standard (>45% Cr). However, achieving high-grade ferrochrome needs enhancement through chromite sand beneficiation before smelting to improve the Cr2O3 content and the chromium-to-iron ratio (Cr: Fe).

KEYWORDS: chromite sand; chromium; ferrochrome; DC submerged arc furnace.

1. Introduction

Chromite is widely utilized, especially in producing ferrochrome, a key material for stainless and alloy steels that provides corrosion resistance and a high-gloss finish [1]. In 300 series stainless steel, the Cr content can reach 25% [2]. The development of the stainless-steel industry has affected the ferrochrome production [3]. Metallurgy chromite use depends heavily on the chromium-to-iron ratio (Cr: Fe). A high Cr: Fe ratio determines the ferrochrome production with a high Cr content [4,5]. Specifically, a Cr ratio above 2.8 is required for ferrochrome production, ratios above 1.8 are suitable for refractory materials, and lower ratios are used in the chemical industry [6]. The classification of chromite ores is as follows in Table 1.

Table 1. Chromite ores classification [4]

Ore	%Cr_2O_3	Production
rich in chromium	46%	ferrochromium
rich in iron	40-46%	charge chrome and chemical industry
rich in aluminum	60% (Cr_2O_3+Al_2O_3)	refractories

The classification of ferrochrome grades, such as high-carbon, medium-carbon, low-carbon, and charge-grade, based on ISO standard 54481-81 [7], is shown in Table 2.

Table 2. Ferrochrome grade according to ISO standard 54481-81 [7,20].

Grade	% Cr	% C	% Si	% P	% S
High-carbon	45–70	4–10	0–10	<0.05	<0.10
Medium-carbon	55–75	0.5–4	<1.5	<0.05	<0.05
Low-carbon	55–95	0.1–0.5	<1.5	<0.03	<0.03
Charge-grade	53–58	5–8	3–6		

Ferrochrome production, an energy-intensive process, requires 3000–4500 kWh per ton of alloy [8]. However, preheating or pre-reduction techniques can mitigate energy consumption and greenhouse gas emissions [2]. Ferrochrome alloys primarily consist of chromium and iron, with minor impurities like silicon and carbon. Recent studies emphasize the growing challenge of processing low-grade chromite ores, driven by the depletion of high-quality reserves and increasing global demand for stainless steel. The ferrochrome industry has responded by exploring innovations in processing methods, including preheating, reduction techniques, and alternative reductants, to improve energy efficiency and minimize environmental impact [2,9-11].

FeCr demand has increased substantially since the development of stainless steel production. Chromite ore with a chromium oxide (Cr_2O_3) content of 46-48% is generally required to meet steel industry standards [12]. As technological demands increase, high-grade chromite ore supplies have become constrained, emphasizing the need to utilize low-to-medium grade chromite resources [13-15] such as the one used in this study, which contains only 8,50% Cr, which is equal to 12.43% Cr_2O_3. Utilizing low-grade chromite presents significant challenges to achieving the quality and yield needed for ferrochrome production. Pyrometallurgical processes, particularly the Submerged Arc Furnace (SAF), are commonly used to address these challenges in chromite smelting [2,16]. In making ferrochrome, a carbothermic reduction system occurs in SAF or a direct current (DC) arc furnace [2, 17-19]. To overcome the limitations of low-grade chromite, optimizing process parameters, such as basicity, becomes essential for achieving high metal yield and chromium recovery during smelting [21]. Basicity influences both the phase and the melting point of the slag. Basicity is also important in ferrochrome quality and energy consumption [22]. Previous studies, such as the work by Eissa *et al*., have highlighted that adding silica as a flux to adjust the basicity to 0.74, along with 50% stoichiometric coke as a reductant, yielded favorable results, achieving chromium recovery of 82% with a final product containing 66% chromium and 7% carbon, from raw material that containing more than 38% Cr_2O_3 [23]. Similarly, Nurjaman *et al*. (2018) reported that smelting chromite ore with 19.27% Cr content and a basicity of 0.4 (achieved with silica addition) resulted in a chromium recovery of 88.5% and a ferrochrome product with 35.2% chromium [24].

This study examines the effects of varying flux materials (silica and limestone) and the amount of coke used as a reductant in smelting local low-grade chromite ore with 8,50% Cr content. Investigating how these factors influence metal characteristics, yield, elemental recovery, and phase transformations in metal and slag.

2. Materials and Methods

2.1. Materials.

The chromite ore used in this study is a low-grade ore from Morowali, Central Sulawesi, obtained as beach sand. The chemical composition of the chromite ore is detailed in Table 3.

Table 3. Chemical composition of chromite ore.

Element/Compound	Cr (Cr_2O_3)	Fe	Cr_2O_3	MgO	CaO	Al_2O_3	SiO_2
Grade (%)	8.50 (12,43)	8.77	12.43	11.33	7.73	6.04	12.02

The flux materials, such as silica and limestone, were used (Table 4) to adjust the basicity of the smelting process, both crushed to a particle size of 2–3 cm to enhance reactivity. The addition of flux is useful in controlling the melting point or liquid temperature of the gangue components, optimizing the viscosity of the slag so the metal can be separated from the slag during tapping [25-28].

Table 4. Chemical composition of flux materials (Silica and Limestone).

Flux	**Grade (%)**			
	CaO	MgO	Al_2O_3	SiO_2
Limestone	68.593	0.732	0.299	0.323
Silica	0.252	0.539	1.629	95.438

Coke, which acts as the reducing agent, was also crushed to a similar size. The proximate analysis of coke, including its fixed carbon content, is shown in Table 5.

Table 5. Proximate analysis of coke.

Reductant	***Proximate analysis (wt %)***			
	Moisture	Volatile matter	Ash content	Fix carbon
Coke	0.3	0.9	10.6	88.3

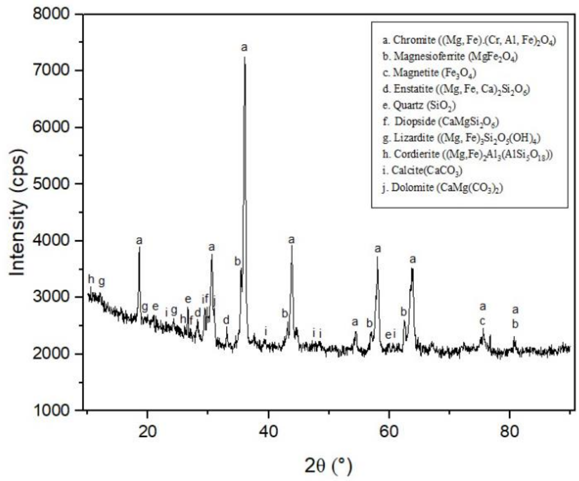

Figure 1. XRD analysis of chromite ore.

Additional characterization of the chromite ore was performed using X-ray diffraction (XRD) and scanning electron microscopy with energy-dispersive X-ray spectroscopy (SEM-EDX) to confirm mineral phases and elemental distribution (Figures 1 and 2).

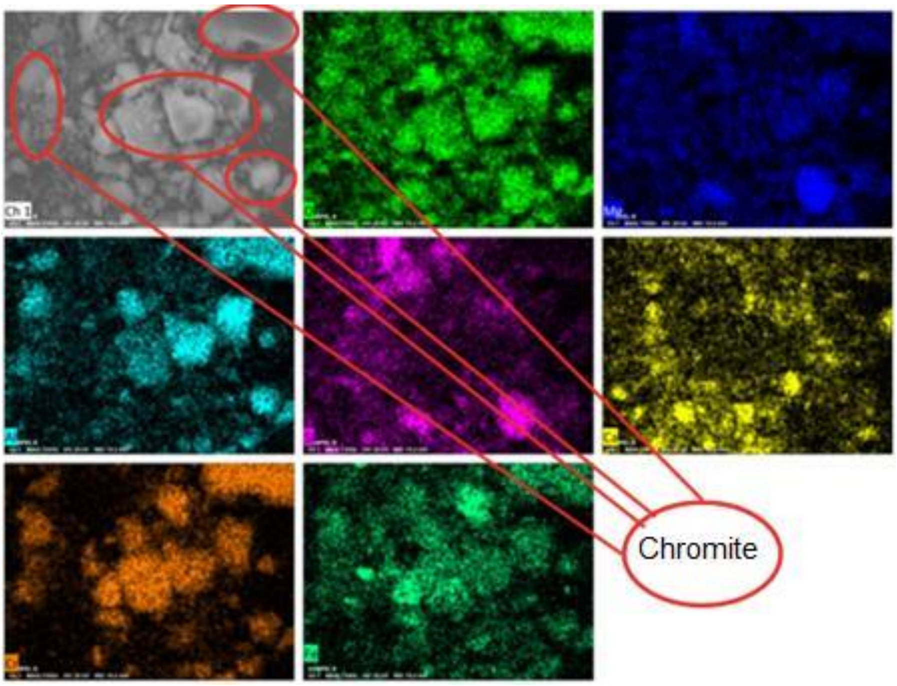

Figure 2. SEM-EDX Mapping analysis of chromite ore.

Coke is introduced into the reduction process as a primary reducing agent, where it reacts with chromite oxides, releasing carbon monoxide gas (CO) and facilitating the reduction of chromium and iron to their metallic forms. The quality of coke is very important in the smelting process because high-content fixed carbon and low-content impurities in coke affect the efficiency of the reduction process [4,27,29]. The amount of coke used directly affects the reduction efficiency and yield of metal in the smelting process, as illustrated by the chemical reactions:

$$FeO + C \rightarrow Fe + CO_{(g)} \quad (1)$$

$$7Cr_2O_3 + 27C \rightarrow 2Cr_7C_3 + 21CO_{(g)} \quad (2)$$

$$Cr_7C_3 + Cr_2O_3 \rightarrow 9Cr + 3CO_{(g)} \quad (3)$$

2.2. Methods.

The chromite sand, crushed fluxes, and coke were pre-analyzed through X-ray Fluorescence (XRF) for its initial chemical composition. The smelting process was conducted in a DC Submerged Arc Furnace on a laboratory scale measuring Ø200 mm × 400 mm. A 60 V, 100 kVA transformer was utilized to convert alternating current (AC) into direct current (DC). The materials were heated to a temperature range of 1200–1433°C. The smelting duration was set to 60 minutes to ensure sufficient reduction and melting of the ore. After smelting, the resulting ferrochrome metal was characterized by XRF to determine the percentage of chromium content and SEM-EDX to examine the microstructure. On the other hand, smelting slag was ground to a particle size of -200 mesh before undergoing XRF analysis for elemental composition and XRD analysis to observe phase transformations.

In this study, flux and coke addition were varied to achieve different levels of basicity and reductant quantities. The basicity values were adjusted by adding varying amounts of limestone and silica flux, as shown in Table 6.

Table 6. Flux addition in smelting with variation in basicity.

Stoichiometry	Basicity	Flux (gram)	
		Limestone	Silica
0.8	0.4	-	900
	0.6	-	425
	0.8	-	180
	1	-	-
	1.2	120	-
	1.4	275	-

The formula to calculate the basicity was $(CaO+MgO)/(SiO_2+Al_2O_3)$ [26,30,31]. The quantity of coke used was also varied, and the corresponding quantities are presented in Table 7.

Table 7. Amount of coke in smelting with variation in reductant quantity.

Stoichiometry	Basicity	Coke (gram)
0.6	Optimal Basicity	98
0.8		131
1		164
1.2		197

Characterization testing on the smelting products evaluated chromium recovery, metal yield, and chromium content in the final ferrochrome product. Oxide compounds in the slag were further examined to determine their phase structure and stability under various smelting conditions.

3. Results and Discussion

3.1. Effect of flux on chromite sand smelting.

The recovery data, as shown in Figure 3(A), indicate that variations in basicity influence the recovery of iron (Fe) and chromium (Cr), as well as the metal yield, because of the role of flux material in binding impurities in the form of slag. The optimal basicity is 0.6 (acidic slag) because it achieved the highest Fe yield of 96.51%, Cr yield of 83.26%, and a total metal yield of 16%. According to Eissa *et al*. [23], high-basicity magnesia slag can slow the smelting process, lowering chromium recovery and metal yield. In contrast, an acidic slag, with a basicity ratio of 0.74, leads to higher chromium recovery and metal yield. According to Kumar [8], the optimal basicity for all cases is close to 1. The higher the basicity, the viscosity will increase due to the higher liquid temperature. High slag viscosity will decrease the reduction reaction, and separating metal from slag will be more difficult when tapping [8]. This finding supports the results obtained in this study, where high magnesia content requires additional silica (SiO_2) to maintain an optimal acidic environment. Figure 3(B) further illustrates that Fe, Cr, and Si content in the ferrochrome product remains relatively stable across different basicity values, indicating that flux addition primarily impacts metal yield and recovery rather than metal composition.

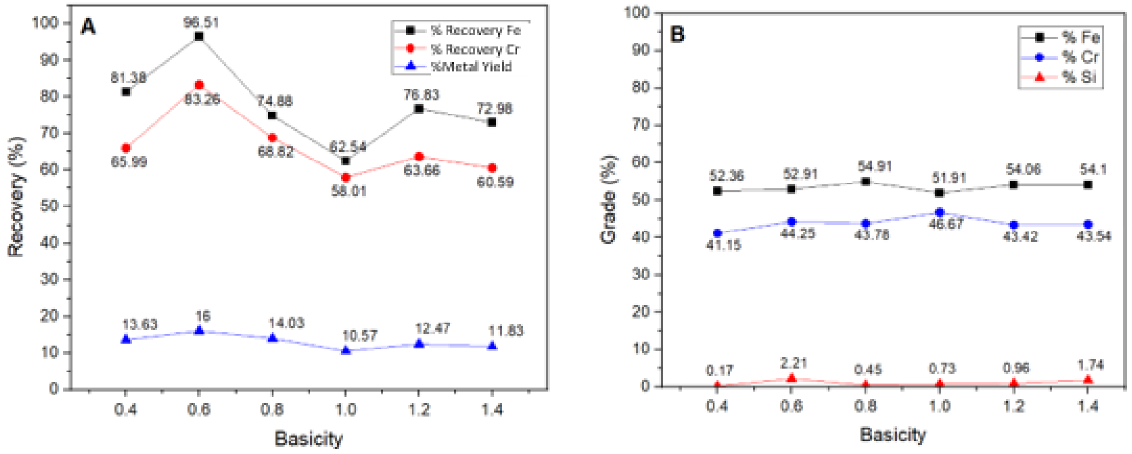

Figure 3. (A) recovery of Fe Cr and metal yield (%) from the smelting process at various basicity variations; **(B)** element content in the ferrochrome metal from the smelting process with various basicity variations.

Table 8 presents the metal content and the oxide compound composition of slag at different basicity levels.

Table 8. Chemical composition of slag compounds.

Stoichiometry	Basicity	Slag (%)					
		Fe	Cr	CaO	MgO	SiO_2	Al_2O_3
0.8	0.4	1.38	2.93	12.43	12.99	40.83	15.93
	0.6	2.04	4.00	16.53	15.92	35.34	20.15
	0.8	3.01	7.41	10.19	13.26	25.75	17.35
	1	3.32	11.71	11.75	13.65	15.78	12.75
	1.2	1.16	3.35	20.53	8.44	28.37	20.59
	1.4	3.42	11.98	16.81	10.81	13.36	12.85

Basicity values below 1, adjusted by adding silica as a flux material, resulted in acidic slag, while values above 1, achieved with limestone addition, created alkaline slag. These oxide compositions are plotted in a Ternary Diagram (Figure 4) to identify the phase formations within the slag.

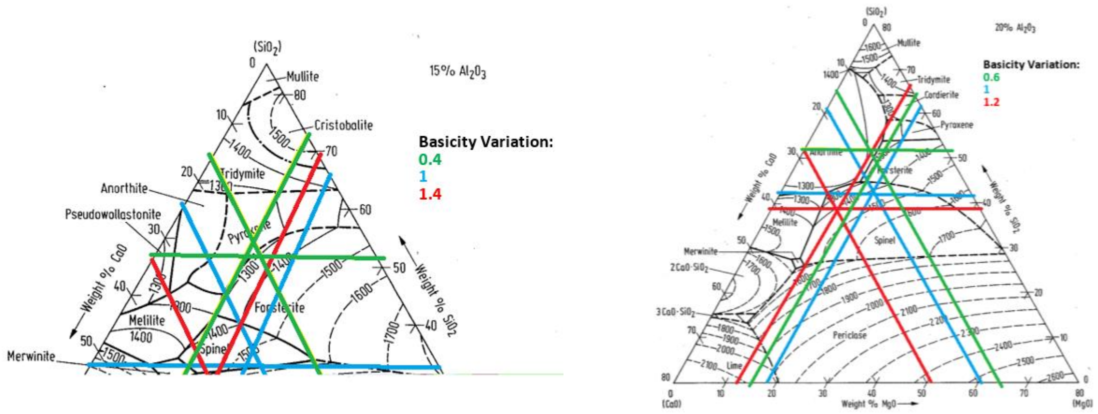

(a) (CaO+MgO+SiO_2 = 0,85); 15%Al_2O_3 **(b)** (CaO+MgO+SiO_2 = 0,8); 20%Al_2O_3

Figure 4. Quadrant basicity ternary diagram **(a)** 15% Al_2O_3; **(b)** 20% Al_2O_3

From Figure 4, it can be observed that increasing basicity also increases the slag's melting point [25]. For instance, the 0.6 basicity variation lies within the iron-rich forsterite (ferroan) phase with a melting point exceeding 1300°C, which is higher than chromite's melting point. At higher basicities (1 and 1.2), the slag phase shifts towards the spinel structure, with melting points above 1400°C. Iron reduction from the forsterite phase becomes more pronounced at these elevated temperatures. Additionally, the formation of the forsterite phase in 0.6 basicity variation is attributed to silica addition, which reacts with Mg in the slag to form Mg_2SiO_4. These high-melting-temperature phases may require additional energy, which could impact the efficiency of the reduction process.

XRD analysis (Figure 5) of slag further supports these observations, showing the formation of forsterite (Mg_2SiO_4), fayalite (Fe_2SiO_4), and spinel ($MgAl_2O_4$) phases at varying basicities. In the 0.6 basicity variation, only Forsterite (Mg_2SiO_4) and Fayalite (Fe2SiO4) are formed, without the presence of Spinel ($MgAl_2O_4$). Meanwhile, spinel is formed at a basicity of 1.0 and 1.2, which is a compound with a high melting point. A higher temperature is needed for compounds with a high melting point to obtain a low viscosity, and the melting process can occur perfectly. Because the metal alloy is heated within the liquid slag phase, the smelting temperature of slag must be higher than the temperature in metal alloy [32], around 100°C above the liquid, so that the separation of slag and metal can occur perfectly [33]. With a high melting point, spinel can inhibit the melting process, thereby affecting recovery and the resulting metal yield.

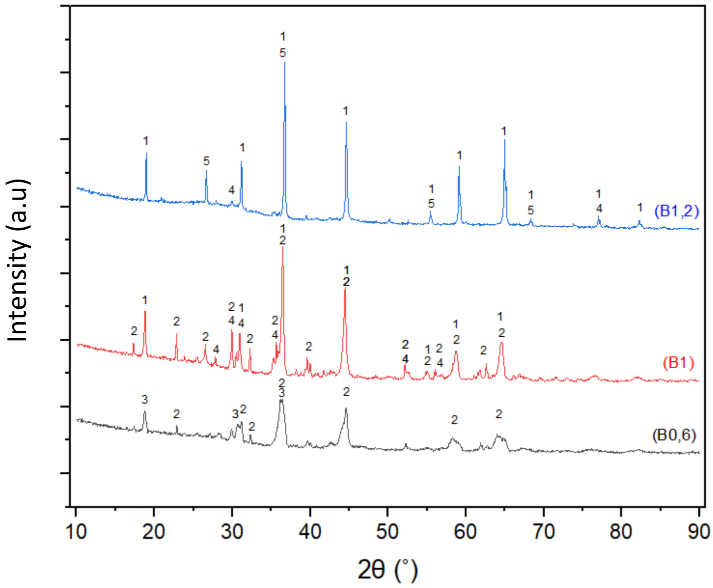

Figure 5. XRD analysis of smelting slag with varying basicity 0.6, 1 and 1.2: 1-Spinel ($MgAl_2O_4$), 2- Forsterite (Mg_2SiO_4), 3- Fayalite (Fe_2SiO_4), 4-Diopside ($CaMg(SiO_3)_2$), 5-Quartz Low (SiO_2).

The predominance of spinel phases at higher basicities suggests that chromium reduction also follows as iron is reduced, leading to residual impurities in the form of spinel (M_3O_5) [34]. Thus, based on the characterization tests, basicity of 0.6 with silica addition was found to yield the most favorable chromium recovery and metal yield.

Based on the Ellingham Diagram, the melting points of Fe and Cr are below 1300°C. Owing to the smelting process temperature range from 1200–1433°C, Fe and Cr reduce and form a liquid phase that settles at the furnace's bottom due to its higher density than slag. The SEM-EDX test results (Figure 6) show that the resulting metal contains silica (Si) traces. However, silica was also partially reduced and incorporated into the metal because of the high temperatures near the arc (graphite electrode), which can exceed 1800°C. This elevated temperature caused the silica, which has a melting point above 1620°C, to reduce and combine with the metal. The remaining silica formed slag phases such as forsterite (Mg_2SiO_4), low quartz (SiO_2), fayalite (Fe_2SiO_4), and diopside ($CaMg(SiO_3)_2$). According to Ringdalen, in

Submerged Arc Furnace technology, most of the rapid reduction occurs near the graphite electrode tip [35].

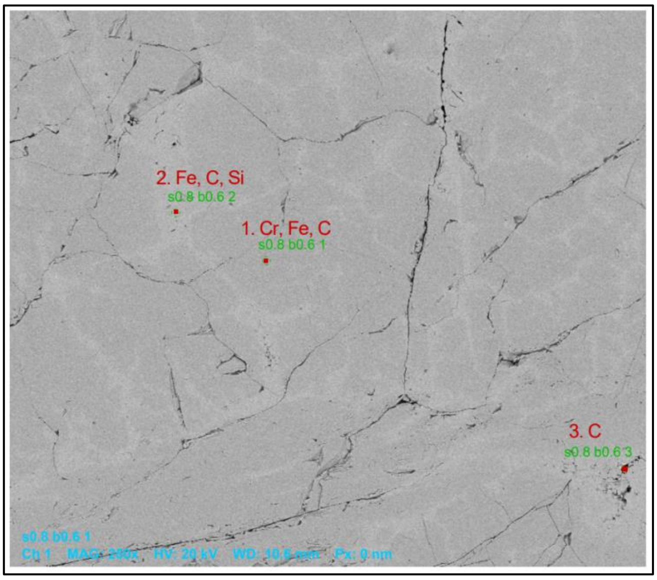

Figure 6. SEM-EDX analysis of ferrochrome metal with basicity variation 0.6: 1 (Cr, Fe, C), 2 (Fe, C, Si), 3 (C).

3.2. Effect of coke addition on chromite sand smelting.

Figure 7(A) depicts the effect of varying stoichiometric ratios of coke on metal yield and chromium recovery. The optimal stoichiometric ratio was 1.2, resulting in a metal yield of 18.33%, chromium recovery of 98.72%, and iron recovery of 95.17%. Figure 7(B) shows that the metal's elemental composition of Cr and Fe remains stable across different stoichiometric ratios, indicating that variations in reductant amount mainly influence yield and recovery rather than the metal’s elemental composition. However, at a stoichiometric ratio of 1.2, there was an observed increase in Si content (up to 7%), which is attributed to higher melting temperatures at this reductant level. When an additional 20% stoichiometry increased the amount of reductant, the metal recovery and yield reached optimal levels, as illustrated in Figure 7(B). According to Eissa *et al*., adding coke as a reductant significantly impacts chromium recovery and metal yield [23].

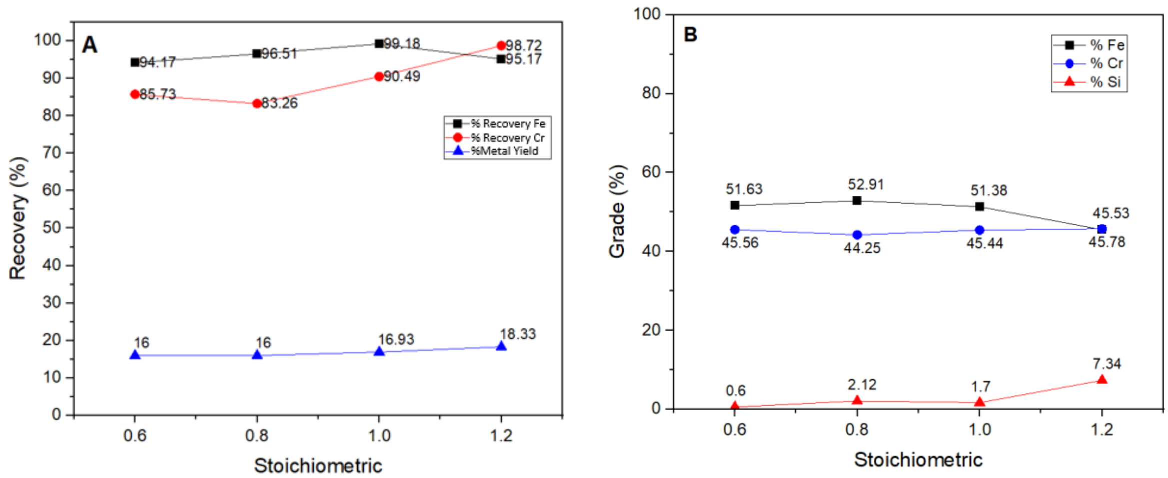

Figure 7. (A) Recovery of Fe and Cr and the metal yield (%) from the smelting process at different stoichiometric variations; **(B)** The elemental content in the ferrochrome metal results from the smelting process at different stoichiometric variations.

XRD analysis of slag (Figure 8) with varying stoichiometric ratios reveals that coke addition does not significantly alter the phase structure in the slag, as the basic system of CaO-MgO-SiO_2-Al_2O_3 remains consistent. However, differences in intensity in the diffractograms reflect higher phase concentrations at increased silica rock levels.

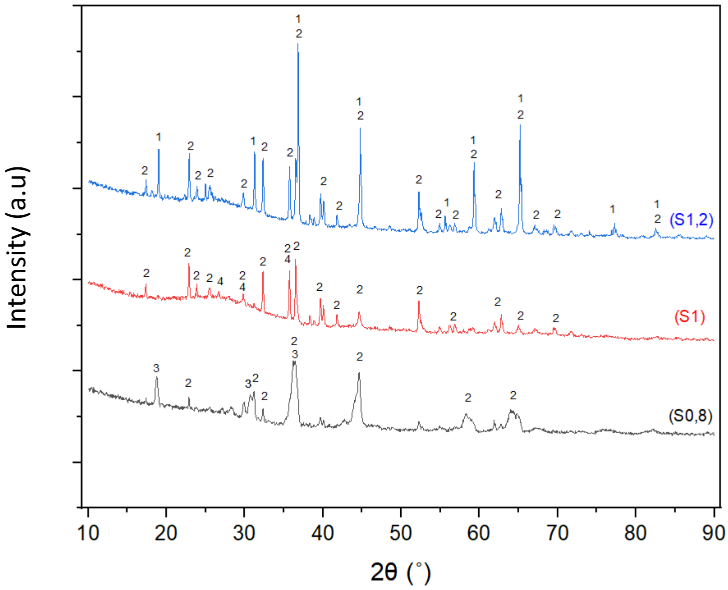

Figure 8. XRD analysis of smelting slag with varying stoichiometry; 1-Spinel ($MgAl_2O_4$), 2- Forsterite (Mg_2SiO_4), 3- Fayalite (Fe_2SiO_4), 4-Diopside ($CaMg(SiO_3)_2$), 5-Quartz Low (SiO_2).

Figure 9 shows that the produced ferrochrome metal has a chromium content of approximately 46%. Ferrochrome with a chromium content of 45-70% and carbon (C) content between 4-10% is classified as High Carbon Ferrochromium [7,20]. In this study, the melting process occurred within a temperature range of 1200–1433°C, with temperatures monitored using a thermocouple at the 50-minute mark of the smelting process. However, reduction reactions near the graphite electrode likely occurred at temperatures exceeding 1800°C.

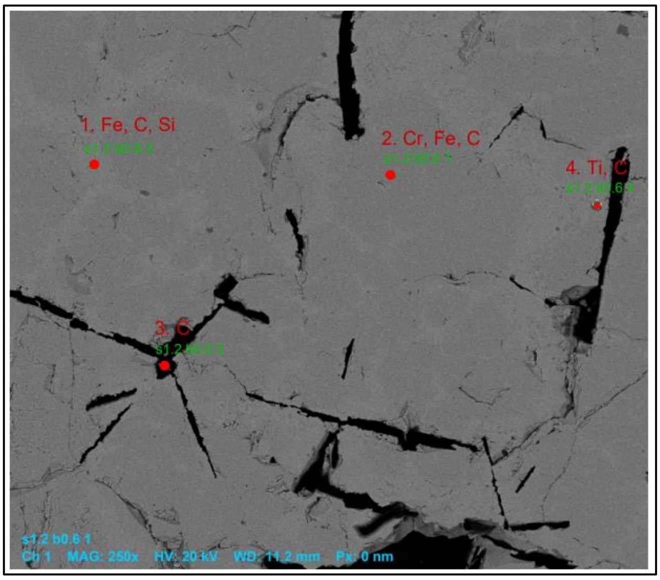

Figure 9. SEM-EDX analysis of ferrochrome metal with stoichiometric variation 1.2; 1 (Fe, C, Si), 2 (Cr, Fe, C), 3 (C), 4(Ti, C).

At these high temperatures, chromium carbide (Cr_7C_3) may form within the ferrochrome, as suggested by Goel [36], who noted that carbothermic reduction of chromite with coke yields pure chromium at temperatures above 1800°C. In contrast, chromium carbide forms at 1250–1600°C.

In this study, based on SEM-EDS, no chromium carbide was found. If chromium carbide is formed, the carbon content will increase, and ferrochrome will be formed with a high C content. Meanwhile, the standard C content for high-carbon ferrochromium is limited, about 4-10% [7,20]. If the carbon content produced is excessive, further processes are needed to reduce the amount of carbon so that the ferrochrome production process will not be economical.

The SEM-EDX analysis also detected small amounts of silica (Si) and titanium (Ti) in the metal. According to Ringdalen [35], in Submerged Arc Furnace technology, rapid reduction primarily occurs near the tip of the graphite electrode, where temperatures can exceed 1800°C, facilitating partial reduction of elements with high melting points. Ít causes silica, with a melting point above 1650°C, and titanium, also melting above 1650°C, to partially reduce in the high-temperature arc flame area, allowing these elements to incorporate into the ferrochrome.

4. Conclusions

The study demonstrates that acidic slag (basicity 0.6) achieved by adding silica flux produces the highest metal recovery and yield, with chromium recovery of 83.26% and a metal yield of 16%. Adding 20% stoichiometric coke as a reductant further improved reduction rates during smelting, achieving optimal chromium recovery and metal yield of 98.72% and 18.33%, respectively. The ferrochrome product with 45.78% Cr meets the minimum low-grade ferrochrome standard (>45% Cr). However, achieving high-grade ferrochrome requires further concentration of chromite sand using some methods such as physical beneficiation or reduction-roasting, which enhance the Cr_2O_3 content and improve the chromium-to-iron ratio (Cr: Fe).

Author Contributions

Conceptualization, F.N.; methodology, B.S., F.N. and U.H.; software, M.R.A.F., M.S.P.Z., F.M. and F.N.; validation, U.H. and F.N.; formal analysis, M.R.A.F., M.S.P.Z., F.M., F.N. and U.H.; investigation, M.R.A.F., F.N. and U. H.; resources, F.N. and U.H.; data curation, M.R.A.F., M.S.P.Z., F.M., F.N. and U.H.; writing—original draft preparation, M.R.A.F.; writing—review and editing, U.H., A.S.H. and F.N.; visualization, M.R.A.F. and U.H.; supervision, B.S., L.O.A., H.Z.H., A.J., D.D.; project administration, U.H.; funding acquisition, U.H. and F.N.. All authors have read and agreed to the published version of the manuscript."

Institutional Review Board Statement

Not applicable.

Informed Consent Statement

Not applicable.

Data Availability Statement

Data supporting the findings of this study are available upon reasonable request from the corresponding author.

Funding

This research was partially funded by a 2024 research grant from the Research Organization for Nanotechnology and Materials under the National Research and Innovation Agency of Indonesia (BRIN).

Acknowledgments

The authors thank the Research Center for Mining Technology – National Research and Innovation Agency of Indonesia for providing research facilities. Appreciation is also extended to Universitas Indonesia and Institut Teknologi Sumatera for their technical support. The authors acknowledge the contributions of Mr. Bambang Suharno from the Department of Metallurgy and Materials at Universitas Indonesia and Mr. Fajar Nurjaman from the Research Center for Mining Technology – National Research and Innovation Agency of Indonesia as promotor and co-promotor for their support in this research.

Conflicts of Interest

The author confirms that there are no known financial conflicts of interest or personal relationships that could have been perceived as influencing the work presented in this paper.

References

1. Hjartarson, J.; McGuinty, L.; Boutilier, S.; Beneath the Surface: Uncovering the Economic Potential of Ontario's Ring of Fire. Majernikova, E., Ed.; Ontario Chamber of Commerce, Ontario, Canada: **2014**.
2. Wei, W.; Samuelsson, P.B.; Jönsson, P.G.; Gyllenram, R.; Glaser, B. Energy Consumption and Greenhouse Gas Emissions of High-Carbon Ferrochrome Production. *JOM* **2023**, *75*, 1206-1220, https://doi.org/10.1007/s11837-023-05707-8.
3. Singha, P.; Das, S.; Kundu, S.; Majumdar, K.; Singh, A.; Paliwal, M. Ferrochrome Production in a Submerged Electric Arc Furnace: Fundamental Analysis Based upon the FactSage-Macro Program Approach. *Steel Res. Int.* **2024**, *95*, 2300840, https://doi.org/10.1002/srin.202300840.
4. Downing, J.H.; Deeley, P.D.; Fichte, R. Chromium and Chromium Alloys. In Ullmann's Encyclopedia of Industrial Chemistry; Wiley: **2000**, https://doi.org/10.1002/14356007.a07_043.
5. Abdalla, A.; Mohanty, S.R.; Yadav, S.; Shukla, A.K.; Bhalla, A. Assessment of Zero Waste Approach by Enhancing Chromium-to-Iron Ratio in Chromite Ore Through Magnetizing Roasting: A Novel Comparative Sustainable Study of Conventional and Hybrid Microwave Heating Methods. *J. Sustain. Metall.* **2024**, *10*, 2398-2416, https://doi.org/10.1007/s40831-024-00924-0.
6. Murthy, Y.R.; Tripathy, S.K.; Kumar, C.R. Chrome ore beneficiation challenges & opportunities – A review. *Miner. Eng.* **2011**, *24*, 375-380, https://doi.org/10.1016/j.mineng.2010.12.001.
7. du Preez, S.P.; van Kaam, T.P.M.; Ringdalen, E.; Tangstad, M.; Morita, K.; Bessarabov, D.G.; van Zyl, P.G.; Beukes, J.P. An Overview of Currently Applied Ferrochrome Production Processes and Their Waste Management Practices. *Minerals* **2023**, *13*, 809, https://doi.org/10.3390/min13060809.
8. Kumar, P.; Nilamadhaba, S.; Aditya, R.; Narayan, R.B.; and Tripathy, S.K. Influence of process parameters on impurity level in ferrochrome production-An industrial-scale analysis. *Miner. Process. Extr. Metall. Rev.* **2022**, *43*, 622-632, https://doi.org/10.1080/08827508.2021.1913154.
9. Zhumagaliev, Y.; Yerekeyeva, G.; Nurumgaliyev, A.; Mongolkhan, O.; Davletova, A.; Sagynbekova, G. Thermodynamic-diagram analysis of the Fe-Si-Al-Cr system with the construction of diagrams of phase relations. *Metalurgija* **2022**, *61*, 825-827.

10. Letaba, P.S.; Zulu, S. The development of a technology roadmap for ferrochrome producers. *S. Afr. J. Ind. Eng.* **2021**, *32*, 100–109, https://doi.org/10.7166/32-2-2495.
11. Heikkinen, E.-P.; Heikkilä, A.; Vallo, K.; Ikäheimonen, T.; Fabritius, T. A computational study on the mixing and reduction of slags from ferrochrome and stainless steel production. *Calphad* **2021**, *75*, 102349, https://doi.org/10.1016/j.calphad.2021.102349.
12. Tripathy, S.K.; Singh, V.; Ramamurthy, Y. Improvement in Cr:Fe Ratio of Indian Chromite Ore forFerro Chrome Production. *Int. J. Min. Eng. Miner. Proc.* **2012**, *1*, 101–106, https://doi.org/10.5923/j.mining.20120103.01.
13. Koleli, N.; Demir, A. Chapter 11 - Chromite. In Environmental Materials and Waste, Prasad, M.N.V., Shih, K., Eds.; Academic Press: **2016**; pp. 245-263, https://doi.org/10.1016/B978-0-12-803837-6.00011-1.
14. Balangao, J.K.B.; Podiotan, F.J.C.; Ambolode, A.E.C.; Anacleto, N.M. Isothermal reduction smelting of mixed chromite-laterite samples with coconut charcoal as reductant under argon atmosphere in a vertical electric arc furnace. *Int. J. Mech. Eng. Technol.* **2022**, *13*, 46-53, https://doi.org/10.17605/OSF.IO/9YCRE.
15. Shabanov, E.Z.; Saulebek, Z.K.; Akhmetov, A.S.; Mukhtarkhanova, G.K. Smelting of High-Carbon Ferrochromium from Pre-Reduced Chromite Raw Materials. *CIS Iron Steel Rev.* **2024**, *27*, 15-19, https://doi.org/10.17580/cisisr.2024.01.03.
16. Hockaday, S.A.C.; Bisaka, K. Some aspects of the production of ferrochrome alloys in pilot dc arc furnaces at Mintek. The Proceedings of The Twelfth International Ferroalloys Congress, Sustainable Future, Helssinki, Finland, June 6-9, 2010; Vartiainen, A., Oyj, O., Ed., Ooutotec Oyj: Finland, **2010**; pp. 367–376.
17. Kumar, P.; Patra, S.K.; Tripathy, S.K.; Sahu, N. Efficient utilization of nickel rich Chromite Ore Processing Tailings by carbothermic smelting. *J. Clean. Prod.* **2021**, *315*, 128046, https://doi.org/10.1016/j.jclepro.2021.128046.
18. Oterdoom, H.; Reuter, M.; Zietsman, J. DC Ferrochrome Smelting: The Arcing Zone and Its Influence on Energy Transport and Exergy Dissipation. *Metall. Mater. Trans. B* **2025**, *56*, 890-912, https://doi.org/10.1007/s11663-024-03365-y.
19. Yu, Y.; Li, B.; Liu, Z.; Qi, F.; Liu, C.; Rong, W.; Kuang, S. Analysis of Electrical Energy Consumption in a Novel Direct Current Submerged Arc Furnace for Ferrochrome Production. *Metall. Mater. Trans. B* **2023**, *54*, 2370-2382, https://doi.org/10.1007/s11663-023-02838-w.
20. Kleynhans, E.L.J.; Beukes, J.P.; Van Zyl, P.G.; Kestens, P.H.I.; Langa, J.M. Unique challenges of clay binders in a pelletised chromite pre-reduction process. *Miner. Eng.* **2012**, *34*, 55-62, https://doi.org/10.1016/j.mineng.2012.03.021.
21. Mills, K.C. Basicity and optical basicities of slags. In Slag Atlas, 2nd Edition; Verein Deutscher Eisenhüttenleute, Ed.; Verlag Stahleisen GmbH: Düsseldorf, Germany, **1995**; pp. 9–19.
22. Hu, T.; Liu, H.; Liu, B.; Dai, L.; Zhang, L.; Guo, S. Review on Preparation of Medium- and Low-carbon Ferrochrome Alloys. In Proceedings of the 10th International Symposium on High-Temperature Metallurgical Processing;Springer, Cham, **2019**; pp. 349-359, https://doi.org/10.1007/978-3-030-05955-2_33.
23. Eissa, M.; El-Farmawy, H. Carbothermic smelting of high carbon ferrochromium alloy from low and high grade chromite ores. *Ironmak. Steelmak.* **2012**, *39*, 31-37, https://doi.org/10.1179/1743281211Y.0000000047.
24. Nurjaman, F.; Subandrio, S.; Ferdian, D.; Suharno, B. Effect of basicity on beneficiated chromite sand smelting process using submerged arc furnace. *AIP Conf. Proc.* **2018**, *1964*, 020009, https://doi.org/10.1063/1.5038291.
25. Geldenhuys, I.J. Pilot plant smelting of canadian and south african chromite in a dc furnace. *Proceeding of the 59th Conference of Metallurgists, COM 2020: The Canadian Institute of Mining, Metallurgy and Petroleum*, virtual online conference, October 14-15 2020; **2020**.
26. Güney, H.; Güner, Ö.; Boncuk, F.F.; Kan, S.; Benzeşik, K.; Yücel, O. A Decarbonization Approach for FeCr Production. *J. Sustain. Metall.* **2023**, *9*, 216-229, https://doi.org/10.1007/s40831-022-00632-7.
27. Sahu, N.; Tripathy, S.K.; Rath, U.P.; Rout, B.N.; Roshan, A.; Kapure, G.U.; Biswas, A. Characterization of Chromiferrous Pyroxenite and Its Application as Flux in Ferrochrome Production Through an Industrial-Scale Submerged Arc Furnace. *J. Sustain. Metall.* **2022**, *8*, 1650-1661, https://doi.org/10.1007/s40831-022-00591-z.
28. Tangstad, M.; Beukes, J.P.; Steenkamp, J.; Ringdalen, E. 14 - Coal-based reducing agents in ferroalloys and silicon production. In New Trends in Coal Conversion, Suárez-Ruiz, I., Diez, M.A., Rubiera, F., Eds.; Woodhead Publishing: **2019**; pp. 405-438, https://doi.org/10.1016/B978-0-08-102201-6.00014-5.

29. Ye, L.; Peng, Z.; Tian, R.; Tang, H.; Anzulevich, A.; Rao, M.; Li, G. Efficient pre-reduction of chromite ore with biochar under microwave irradiation. *Sustain. Mater. Technol.* **2023**, *37*, e00644, https://doi.org/10.1016/j.susmat.2023.e00644.
30. Luo, J.; Hou, S.; Rao, M.; Liang, G.; Li, G.; Jiang, T. Enhanced Chromium Recovery in the Smelting of Ferronickel Along with Energy-Saving: An Industrial Case Study. *JOM* **2022**, *74*, 178-184, https://doi.org/10.1007/s11837-021-05001-5.
31. Bin Tasnim, T.; Tafaghodi Khajavi, L. Chromium Stabilization in Ferrochromium Slag for its Utilization as Aggregate Material. *J. Sustain. Metall.* **2022**, *8*, 1041-1052, https://doi.org/10.1007/s40831-022-00542-8.
32. Panigrahi, M.; Ganguly, R.I.; Dash, R.R. Fundamentals of Ferrochrome (FeCr) Alloy and Its Slag. In High Electrical Resistant Materials: Ferrochrome Slag Resource Ceramics; Panigrahi, M., Ganguly, R.I., Dash, R.R., Eds.; Scrivener Publishing LLC: USA, **2024**; pp. 1-61, https://doi.org/10.1002/9781394231287.ch1.
33. Bhalla, A.; Shukla, A.K. Overview of thermodynamics concepts in production of some ferroalloys (ferrochrome, ferromanganese, ferrotitanium and ferrovanadium). Processing of THANOS International Conference 2022, 2 day hybrid conference, September 28-29, 2022; South African Institute of Mining and Metallurgy: South Africa, **2022**; pp. 11–21.
34. Hayes, P.C. Aspects of SAF smelting of ferrochrome. Proceedings of the Tenth International Ferroalloys Congress. Cape Town, South Africa, February 1-4, 2004; South African Institute of Mining and Metallurgy: South Africa, **2004**; Volume 10, pp. 14.
35. Ringdalen, E. The High Carbon Ferrochromium Process, Reduction Mechanisms. Thesis, NTNU, Trondheim, Norway, **1999**; pp. 149-167.
36. Goel, R. Smelting Technologies for Ferrochromium Production-Recent Trends. In Ferro Alloy Industries in the Liberalised Economy, Vaish, A.K.; Singh, S.D.; Goswami, N.G.; Ramachandrarao, P., Eds.; NML Jamshedpur: India, **1997**; pp. 37–50.

Publisher's Note & Disclaimer